BIOMOLECULES & THERAPEUTICS

Original Article
Biomol Ther 24(1), 75-84 (2016)

Rosmarinic Acid Attenuates Cell Damage against UVB Radiation-Induced Oxidative Stress via Enhancing Antioxidant Effects in Human HaCaT Cells

Pattage Madushan Dilhara Jayatissa Fernando[1], Mei Jing Piao[1], Kyoung Ah Kang[1], Yea Seong Ryu[1], Susara Ruwan Kumara Madduma Hewage[1], Sung Wook Chae[2] and Jin Won Hyun[1,*]

[1]Department of Biochemistry, School of Medicine, Jeju National University, Jeju 63243,
[2]Aging Research Center, Korea Institute of Oriental Medicine, Daejeon 34054, Republic of Korea

Abstract

This study was designed to investigate the cytoprotective effect of rosmarinic acid (RA) on ultraviolet B (UVB)-induced oxidative stress in HaCaT keratinocytes. RA exerted a significant cytoprotective effect by scavenging intracellular ROS induced by UVB. RA also attenuated UVB-induced oxidative macromolecular damage, including protein carbonyl content, DNA strand breaks, and the level of 8-isoprostane. Furthermore, RA increased the expression and activity of superoxide dismutase, catalase, heme oxygenase-1, and their transcription factor Nrf2, which are decreased by UVB radiation. Collectively, these data indicate that RA can provide substantial cytoprotection against the adverse effects of UVB radiation by modulating cellular antioxidant systems, and has potential to be developed as a medical agent for ROS-induced skin diseases.

Key Words: Antioxidant system, Oxidative stress, Reactive oxygen species, Rosmarinic acid, Ultraviolet B

INTRODUCTION

Ultraviolet (UV) radiation is a key risk factor that facilitates the initiation and development of various skin diseases (Park *et al*., 2013). Solar UV radiation on the earth's surface consists of approximately 90-99% UVA and 1-10% UVB. UVA (320-400 nm) is a thousand times less capable of causing sunburn than UVB (Avila *et al*., 2014). UVB (280-320 nm), which is largely absorbed by the protective ozone layer, penetrates as far as the epidermal basal cell layer of the skin, affecting mainly epidermal cells and thereby acting as a potent genotoxic agent (Avila *et al*., 2014). Exposure of the skin to UVB paves the way for the generation of reactive oxygen species (ROS) such as hydrogen peroxide, superoxide anion, hydroxyl radical, and singlet oxygen (Hanson and Clegg, 2002; Lee *et al*., 2014).

Several lines of evidence show that direct absorption of UVB photons or UVB-induced oxidative stress leads to the formation of cyclobutane pyrimidine dimers and pyrimidine-pyrimidone (6-4) photoproducts and the oxidized products, including protein carbonyls, lipid hydroperoxides and 8-hydroxydeoxyguanosine (Vayalil *et al*., 2004; Verschooten *et al*., 2006). Evidence accumulated in recent years revealed that UVB also affects the level of skin antioxidants, interfering with the skin's ability to protect itself against the reactive nitrogen/oxygen species (Piao *et al*., 2013). However, UVB-induced oxidative stress is naturally counterbalanced by the specific antioxidant system employed by the skin (McArdle *et al*., 2002). Unless human skin maintains its intracellular redox balance, UVB can completely demolish the epidermal defensive antioxidant system, which comprises superoxide dismutase (SOD), catalase (CAT), heme oxygenase-1 (HO-1), and non-enzymatic antioxidants (reduced glutathione, ascorbate, and ubiquinol) (Yoshihisa *et al*., 2014).

A recently developed strategy for cytoprotection against UVB-induced oxidative stress is to support the endogenous antioxidant system of the skin with substances of plant-based origin (Silva *et al*., 2010). Rosmarinic acid (RA) is a water-soluble hydroxylated compound, naturally found in a veriety of medicinally used herbs such as *Rosmarinus officinalis, Orthosiphon stamineus, Orthosiphon diffusus, Artemisia capillaris*, and *Calendula officinalis*. RA is characterized by its antioxidant properties with direct free-radical scavenging activity

Open Access **http://dx.doi.org/10.4062/biomolther.2015.069**

Received Jun 4, 2015 **Revised** Aug 10, 2015 **Accepted** Aug 20, 2015
Published online Jan 1, 2016

***Corresponding Author**
E-mail: jinwonh@jejunu.ac.kr
Tel: +82-64-754-3838, Fax: +82-64-702-2687

(Lee *et al*., 2008).

We designed this study to evaluate the potential role of RA in UVB-induced skin cell damage. Specifically, we attempted to unravel the cytoprotective mechanism of RA against oxidative stress induced by UVB by assessing the status of various antioxidant enzymes.

MATERIALS AND METHODS

Reagents

RA (purity 100%) and CAT antibody were purchased from Santa Cruz Biotechnology (Dallas, TX, USA). 1,1-Diphenyl-2-picrylhydrazyl (DPPH), 2',7'-dichlorodihydrofluorescein diacetate (DCF-DA), 3-(4,5-dimethylthiazol-2-yl)-2,5-diphenyltetrazolium bromide (MTT), N-acetyl-L-cysteine (NAC), Hoechst 33342, 5,5-dimethyl-1-pyrroline-N-oxide (DMPO), and actin antibody were purchased from Sigma-Aldrich Corporation (St. Louis, MO, USA). SOD antibody was purchased from Enzo Life Sciences (Farmingdale, NY, USA), and HO-1 antibody was purchased from Cell Signaling Technology (Danvers, MA, USA). All other chemicals and reagents were of analytical grade.

Cell culture and UVB irradiation

Human keratinocytes (HaCaT cells) obtained from Amore Pacific Company (Yongin, Republic of Korea), were maintained at 37°C in an incubator in a humidified atmosphere of 5% CO_2. The cells were cultured in RPMI 1640 medium containing 10% heat-inactivated fetal calf serum, streptomycin (100 μg/ml), and penicillin (100 U/ml). The UVB source was a CL-1000M UV Crosslinker (UVP, Upland, CA, USA), which was used to deliver an energy spectrum of UVB radiation (280-320 nm; peak intensity, 302 nm), and 30 mJ/cm^2 of UVB was exposed to cells.

Cell viability

Cells were treated with RA (0.625, 1.25, 2.5, or 5 μM) and exposed to UVB radiation 1 h later. They were then incubated at 37°C for 48 h. At this time, MTT was added to each well to obtain a total reaction volume of 200 μl. After 4 h incubation, the supernatant was removed by aspiration. The formazan crystals in each well were dissolved in dimethyl sulfoxide (DMSO; 150 μl), and the absorbance at 540 nm was measured on a scanning multi-well spectrophotometer (Carmichael *et al*., 1987).

DPPH radical detection

RA (0.625, 1.25, 2.5, 5 μM) and 1 mM NAC was added to 0.1 mM DPPH and mixed well. The mixture was incubated for 30 min, after which the amount of residual DPPH was determined by measuring absorbance at 520 nm using a spectrophotometer.

Intracellular ROS detection

The DCF-DA method was used to detect intracellular ROS levels in HaCaT keratinocytes (Rosenkranz *et al*., 1992). Cells were seeded at a density of 1.5×10^5 cells/well in 24-well culture plates. Sixteen hours after plating, cells were treated with RA (0.625, 1.25, 2.5, 5 μM) or 1 mM NAC. After incubation for 30 min, cells were exposed to H_2O_2 (1 mM) and again incubated for 30 min. H_2O_2-treated cells were treated with DCF-DA (25 μM) solution and incubated for another 10 min to detect the fluorescence of DCF. Otherwise, cells were incubated with RA (2.5 μM) or 1 mM NAC for 1 h and exposed to UVB (30 mJ/cm^2). Following 24 h, cells were further incubated with DCF-DA solution for 10 min. Fluorescence of DCF was detected using a PerkinElmer LS-5B spectrofluorometer (Perkin Elmer, Waltham, MA, USA).

Detection of the superoxide anion

The superoxide anion was produced via the xanthine/xanthine oxidase system and reacted with a nitrone spin trap, DMPO. The DMPO/•OOH adducts were detected using a JES-FA electron spin resonance (ESR) spectrometer (JEOL, Tokyo, Japan) (Kohno *et al*., 1994). Briefly, ESR signaling was recorded 5 min after 20 μl of xanthine oxidase (0.25 unit/ml) was mixed with 20 μl each of xanthine (5 mM), DMPO (1.5 M), RA (2.5 μM). The ESR spectrometer parameters were set as follows: magnetic field, 336 mT; power, 1.00 mW; frequency, 9.438 GHz; modulation amplitude, 0.2 mT; gain, 500; scan time, 0.5 min; scan width, 10 mT; time constant, 0.03 sec; and temperature, 25°C.

Detection of hydroxyl radical

The hydroxyl radical was generated via the Fenton reaction (H_2O_2+$FeSO_4$) and reacted with DMPO. The resultant DMPO/•OH adducts were detected using an ESR spectrometer (Li *et al*., 2004). The ESR spectrum was recorded 2.5 min after a phosphate buffer solution (pH 7.4) was mixed with 0.2 ml each of DMPO (0.3 M), $FeSO_4$ (10 mM), H_2O_2 (10 mM), and RA (2.5 μM). The ESR spectrometer parameters were as follows: magnetic field, 336 mT; power, 1.00 mW; frequency, 9.438 GHz; modulation amplitude, 0.2 mT; gain, 200; scan time, 0.5 min; scan width, 10 mT; time constant, 0.03 sec; and temperature, 25°C.

Protein carbonyl formation

Cells were treated with RA at a concentration of 2.5 μM for 24 h. One hour later, cells were exposed to UVB and incubated at 37°C for another 24 h. The extent of protein carbonyl formation was determined using an Oxiselect™ protein carbonyl ELISA kit from Cell Biolabs (San Diego, CA, USA).

Single-cell gel electrophoresis (comet assay)

The degree of oxidative DNA damage was assessed by comet assay (Singh, 2000). A cell suspension was mixed with 70 μl of 1% low-melting agarose (LMA) at 37°C, and the mixture was spread onto a fully frosted microscopic slide precoated with 200 μl of 1% normal melting agarose (NMA). After solidification of the agarose, the slide was covered with another 170 μl of 0.5% LMA, and then immersed in lysis solution (2.5 M NaCl, 100 mM Na-EDTA, 10 mM Tris, 1% Triton X-100, and 10% DMSO, pH 10) for 1 h at 4°C. The slides were subsequently placed in a gel electrophoresis apparatus containing 300 mM NaOH and 10 mM Na-EDTA (pH 10) and incubated for 30 min to allow for DNA unwinding and the expression of alkali-labile damage. An electrical field (300 mA, 25 V) was then applied for 30 min at 25°C to draw the negatively charged DNA towards the anode. The slides were washed three times for 10 min at 25°C in neutralizing buffer (0.4 M Tris, pH 7.5), and then washed once for 10 min at 25°C in 100% ethanol. Then, the slides were stained with 80 μl of 10 μg/ml ethidium bromide and observed using a fluorescence microscope and

image analyzer (Kinetic Imaging, Komet 5.5, UK). Tail length and percentage of total fluorescence in the comet tails were recorded for 50 cells per slide.

Lipid peroxidation assay

Lipid peroxidation was assayed by colorimetric determination of the levels of 8-isoprostane, a stable end product of lipid peroxidation, in medium from HaCaT cells (Beauchamp *et al*., 2002). A commercial enzyme immune assay (Cayman Chemical, Ann Arbor, MI, USA) was employed to detect 8-isoprostane. Lipid peroxidation was also assessed using DPPP as a probe (Okimoto *et al*., 2000). DPPP reacts with lipid hydroperoxides to generate a fluorescent product, DPPP oxide, thereby providing an indication of membrane damage. Cells were treated with 2.5 μM of RA for 1 h, followed by exposure to UVB (30 mJ/cm^2). Twenty-four hours later, cells were incubated with 20 μM DPPP for 30 min in the dark. Images of DPPP fluorescence were captured on a Zeiss Axiovert 200 inverted microscope at an excitation wavelength of 351 nm and an emission wavelength of 380 nm.

Nuclear staining with Hoechst 33342

Cells were treated with 2.5 μM RA and exposed to 30 mJ/cm^2 UVB radiation 1 h later. After incubation for an additional 24 h at 37°C, 1 μl of the DNA-specific fluorescent dye Hoechst 33342 (stock, 15 mM) was added to each well of the 6-well plate. The plate was then incubated for 10 min at 37°C. The degree of nuclear condensation in the stained cells was determined by visualization with a fluorescence microscope equipped with a CoolSNAP-Pro color digital camera.

DNA fragmentation

Cells were treated with RA (2.5 μM) for 24 h. One hour later, the cells were exposed to UVB and incubated at 37°C for another 24 h. Cellular DNA fragmentation was assessed by analyzing cytoplasmic histone-associated DNA fragments using a kit from Roche Diagnostics (Portland, OR, USA).

Western blot analysis

Harvested cells were lysed by incubation on ice for 10 min in 160 μl of lysis buffer containing 120 mM NaCl, 40 mM Tris (pH 8), and 0.1% NP 40. The resultant cell lysates were centrifuged at 13,000×*g* for 5 min. Supernatants were collected, and protein concentrations were determined. Aliquots (each containing 5 μg of protein) were boiled for 5 min and electrophoresed on 12% SDS-polyacrylamide gels. Protein blots of the gels were transferred onto nitrocellulose membranes. Membranes were incubated with an appropriate primary antibody (Cu/Zn SOD, CAT, HO-1, and Nrf2) and further incubated with secondary immunoglobulin G-horseradish peroxidase conjugates. Protein bands were visualized by developing the blots using an enhanced chemiluminescence Western blotting detection kit (Amersham, Buckinghamshire, UK) and exposing the membranes to X-ray film.

SOD activity assay

Cells were seeded in a culture dish at a concentration of 1×10^5 cells/ml; 16 h after plating, the cells were treated with 2.5 μM RA. One hour later, cells were exposed to UVB and incubated at 37°C for an additional 24 h. The cells were then washed with cold PBS and harvested by scraping. The harvested cells were suspended in 10 mM phosphate buffer (pH 7.5) and then lysed on ice by sonicating twice for 15 sec. Triton X-100 (1%) was added to the lysates and incubated for 10 min on ice. The lysates were clarified by centrifugation at 5,000×*g* for 10 min at 4°C to remove cellular debris. The protein content of the supernatant was determined using the Bradford method. Total SOD activity was evaluated by measuring the level of inhibition of epinephrine auto-oxidation (Misra and Fridovich, 1972), as follows. Fifty micrograms of protein was added to 500 mM phosphate buffer (pH 10.2) and 1 mM epinephrine. Epinephrine rapidly undergoes auto-oxidation at pH 10 to produce adrenochrome, a pink-colored product, which was assayed at 480 nm using a UV/vis spectrophotometer in the kinetic mode. SOD inhibits the auto-oxidation of epinephrine. The rate of inhibition was monitored at 480 nm, and the amount of enzyme required to produce 50% inhibition was defined as 1 unit of enzyme activity. Total SOD activity was expressed as units/mg protein.

CAT activity assay

Fifty milligrams of protein was added to 50 mM phosphate buffer (pH 7.0) containing 100 mM H_2O_2, and the mixture was subsequently incubated for 2 min at 37°C. Absorbance at 240 nm was monitored for 5 min; the change in absorbance is proportional to the breakdown of H_2O_2 (Carrillo *et al*., 1991). CAT activity was expressed as units/mg protein.

HO-1 activity assay

Cells were homogenized in 0.5 ml of ice-cold 0.25 M sucrose solution containing 50 mM potassium phosphate buffer (pH 7.4). Homogenates were centrifuged at 200×*g* for 10 min. Supernatants were centrifuged at 9,000×*g* for 20 min, and further centrifuged at 105,000×*g* for 60 min. The pellet was then resuspended in 50 mM potassium phosphate buffer (pH 7.4), and the amount of protein was determined by the Bradford method. A reaction mixture (200 μl) containing 0.2 mM of the substrate hemin, 500 μg/ml of cell lysate, 0.5 mg/ml of rat liver cytosol as a source of biliverdin reductase, 0.2 mM $MgCl_2$, 2 mM glucose-6-phosphate, 1 U/ml glucose-6-phosphate dehydrogenase, 1 mM NADPH, and 50 mM potassium phosphate buffer (pH 7.4) was incubated at 37°C for 2 h. The reaction was stopped with 0.6 ml of chloroform; after extraction, the chloroform layer was measured spectrophotometrically. Bilirubin formation was calculated from the difference in absorption between 464 and 530 nm (Kutty and Maines, 1982).

Immunocytochemistry

Cells plated on coverslips were fixed with 4% paraformaldehyde for 30 min and permeabilized with 0.1% Triton X-100 in PBS for 5 min. Cells were treated with blocking medium (3% bovine serum albumin in PBS) for 1 h and incubated with Nrf2 antibody diluted in blocking medium for 2 h. Immunoreacted primary Nrf2 antibody was detected by a 1:500 dilution of FITC-conjugated secondary antibody (Jackson ImmunoResearch Laboratories, West Grove, PA, USA) for 1 h. After washing with PBS, stained cells were mounted onto microscope slides in mounting medium with DAPI (Vector, Burlingame, CA, USA). Images were collected using the LSM 510 program on a Zeiss confocal microscope.

Statistical analysis

All measurements were performed in triplicate, and all values are expressed as means ± standard error. The results

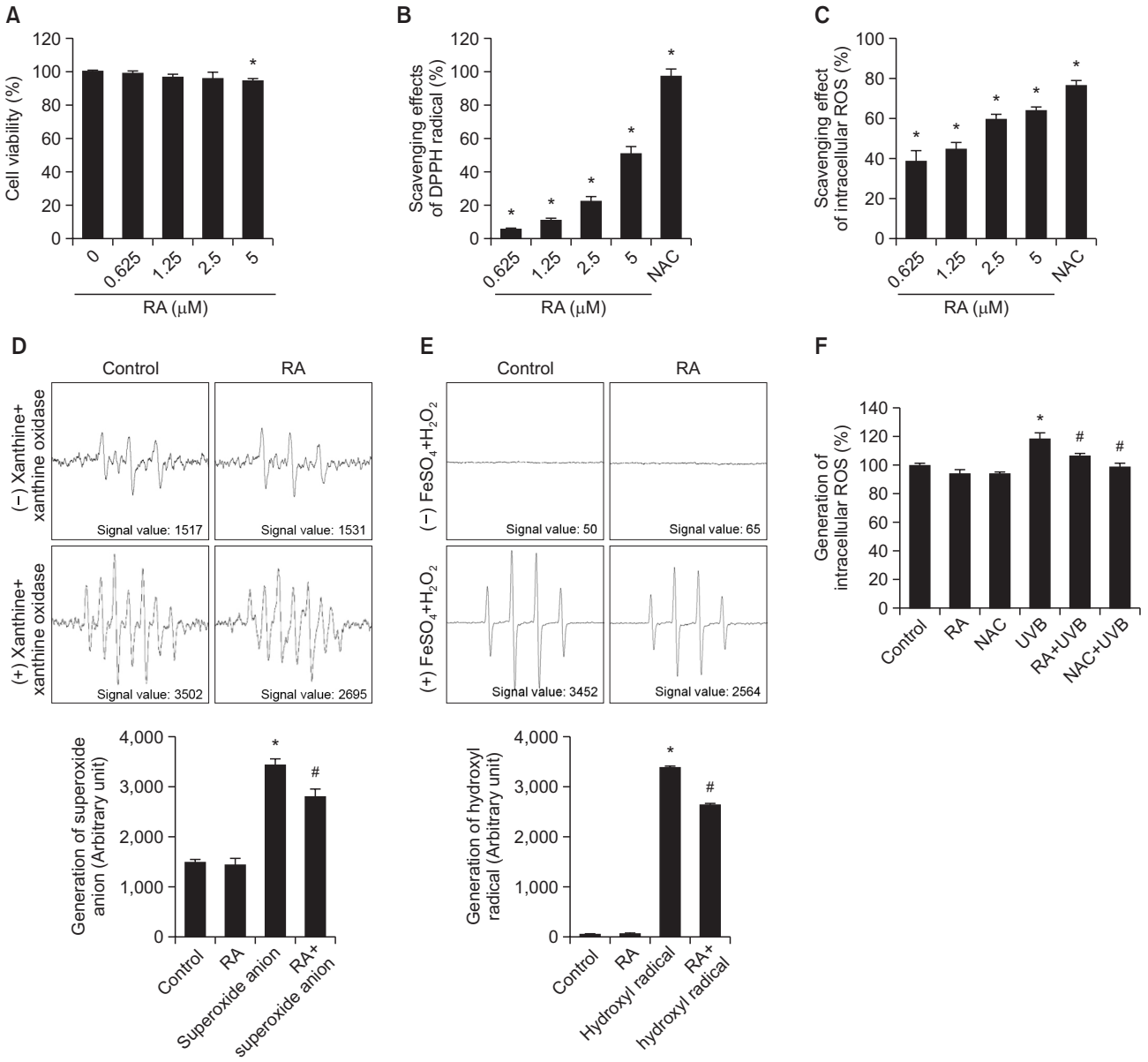

Fig. 1. RA scavenges ROS. (A) HaCaT cells were treated with RA (0, 0.625, 1.25, 2.5, or 5 μM) for 20 h. Cell viability was measured in an MTT assay. (B) Scavenging levels of the DPPH radical were measured spectrophotometrically at 520 nm. NAC (1 mM) served as the positive control. *Significantly different from the control group (p<0.05). (C) The ability of RA to scavenge intracellular ROS generated by H_2O_2 was measured by DCF-DA assay. *Significantly different from control cells (p<0.05). (D) The ability of RA to scavenge superoxide anion was evaluated using the xanthine/xanthine oxidase system. *Significantly different from control (p<0.05); #significantly different from superoxide anion (p<0.05). (E) Ability to scavenge hydroxyl radical was estimated using the Fenton reaction ($FeSO_4$+H_2O_2 system). *Significantly different from control (p<0.05); #significantly different from hydroxyl radical (p<0.05). (F) The ability of RA to scavenge intracellular ROS generated by UVB was evaluated in a DCF-DA assay. *Significantly different from control (p<0.05); #significantly different from UVB-irradiated group (p<0.05).

were subjected to an analysis of variance (ANOVA) using Tukey's test to analyze differences between means. In all cases, p<0.05 was considered to be statistically significant.

RESULTS

RA scavenges free radicals including ROS

Cell viability was approximately >95% at all concentrations of RA used up to 2.5 μM; thus no cytotoxicity was observed (Fig. 1A). RA was tested for its DPPH radical scavenging activity at various concentrations (0.625, 1.25, 2.5, and 5 μM). DPPH radicals were scavenged in a dose-dependent manner; the well-known antioxidant NAC (1 mM) was used as the positive control (Fig. 1B). Subsequently, we measured intracellular ROS scavenging activity by treating cells with H_2O_2 (Fig. 1C). In H_2O_2-treated cells, 2.5 μM RA scavenged 60% of intracellular ROS compared to 77% of intracellular ROS scavenging

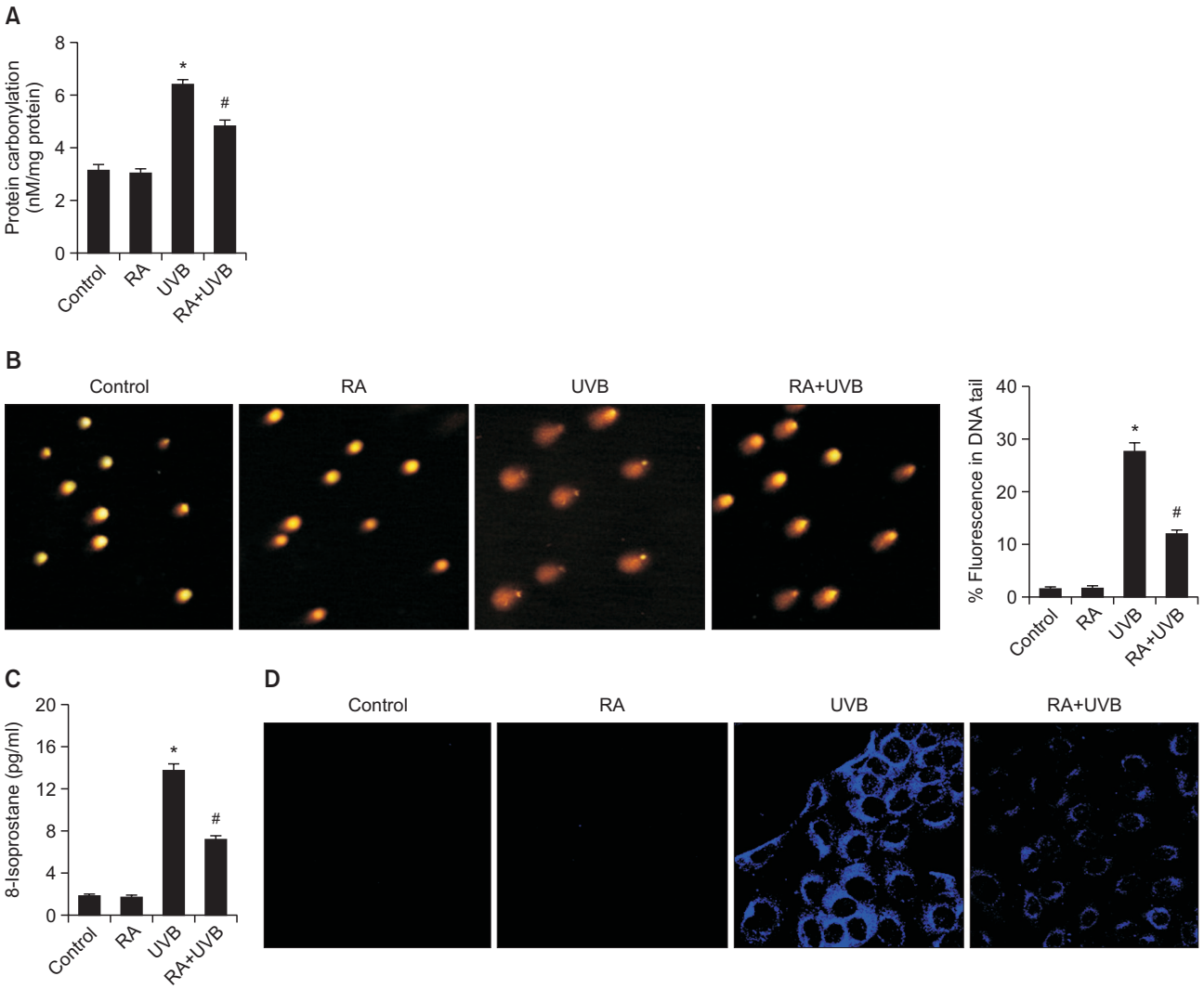

Fig. 2. RA protects HaCaT cells against UVB-induced oxidative protein, DNA, and lipid damage. Cells were treated with 2.5 μM RA for 1 h, and then exposed to UVB radiation. (A) Level of carbonyl formation, a marker of protein oxidation was assessed. *Significant difference from control cells (p<0.05); #significant difference from UVB-irradiated cells (p<0.05). (B) Comet assay was used to assess DNA damage. Representative images and percentages of cellular fluorescence within comet tails are shown. *Significant difference relative to control cells (p<0.05); #significant difference relative to UVB-irradiated cells (p<0.05). (C) Lipid peroxidation was assessed by measuring 8-isoprostane levels in conditioned medium. *Significant difference relative to control cells (p<0.05); #significant difference relative to UVB-irradiated cells (p<0.05). (D) lipid hydroperoxide detection via fluorescence microscopy after the DPPP reaction.

effect in NAC. Based on these results, we chose 2.5 μM as the RA concentration in all subsequent experiments.

Next, we performed ESR spectrometry to measure the superoxide anion and hydroxyl radical scavenging ability of RA via direct quenching of reactive molecules. In the xanthine/xanthine oxidase system, DMPO/•OOH yielded a signal value of 3,502 compared to the 1,517 value of control group, whereas RA decreased the signal value to 2,695 value (Fig. 1D). Correspondingly, in the $FeSO_4$+H_2O_2 system (Fe^{2+}+H_2O_2 → Fe^{3+}+•OH+OH^-), hydroxyl radical caused elevated signal values compared to control cells; however, RA could significantly scavenge these elevated levels of hydroxyl radicals (Fig. 1E). In addition, RA exerted considerable scavenging ability towards ROS generated by UVB (Fig. 1F).

RA attenuates UVB-induced macromolecular damage in HaCaT cells

Intracellular ROS, one of the most destructive products of UVB radiation on the skin, causes damage to cellular macromolecules such as protein, mitochondrial and nuclear DNA, and lipid (Perez-Sanchez *et al*., 2014). Under oxidative stress, carbonyl (CO) groups (aldehyde and ketones) are formed on the side chains of proteins; hence, these chemically stable compounds can be used as biomarkers for oxidative stress (Dean *et al*., 1997). Upon UVB irradiation, protein carbonyl content increased significantly relative to control cells, yet RA significantly prevented the UVB-induced protein carbonyl formation in a significant manner (Fig. 2A).

Accumulating evidence shows that UVB radiation induces a range of DNA damage including single-strand, and double-

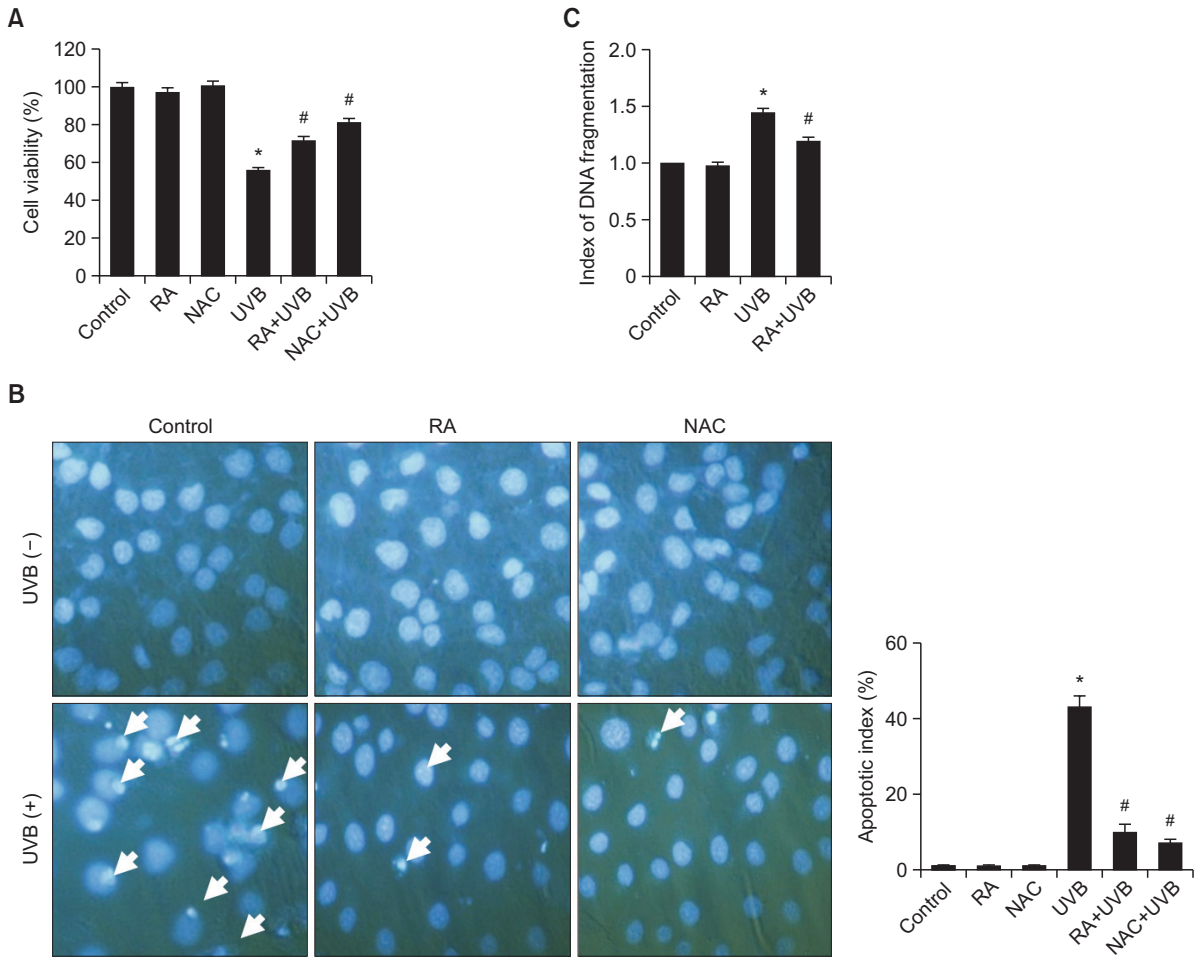

Fig. 3. RA attenuates cells from UVB-induced apoptosis. (A) Cells were pre-treated with 2.5 μM RA or 1 mM NAC, and then exposed to UVB radiation (30 mJ/cm^2). Cell viability was measured in an MTT assay. *Significant difference relative to control cells (p<0.05); #significant difference relative to UVB-irradiated cells (p<0.05). (B) Apoptotic bodies (arrows) were observed by fluorescence microscopy in cells stained with Hoechst 33342 and quantitated. *Significantly different from control (p<0.05); #significantly different from UVB-irradiated cells (p<0.05). (C) DNA fragmentation was analyzed using an enzyme-linked immunosorbent assay kit. *Significantly different from control cells (p<0.05); #significantly different from UVB-irradiated cells (p<0.05).

strand breaks (Horiguchi *et al*., 2001). Damaged cellular DNA can be separated from intact DNA in an electrophoretic field, yielding the classic comet tail. In comparison with controls, cells exposed to UVB irradiation exhibited significantly elongated nuclear tails and elevated percentages of DNA in the tails (Fig. 2B). However, pre-treatment with RA decreased the tail length of UVB-irradiated cells.

ROS induce secretion of 8-isoprostane in HaCaT cells, and the amount of 8-isoprostane in the conditioned medium can be used as a specific index of cellular lipid peroxidation (Beauchamp *et al*., 2002). As demonstrated by Fig. 2C, the concentration of 8-isoprostane was significantly increased in UVB-treated cells, but pre-treatment of cells with RA reversed this increase. In addition, we determined the level of cellular lipid peroxidation by the fluorescence intensity of DPPP oxide, which is formed by the reaction of DPPP with hydroperoxide (Okimoto *et al*., 2000). The fluorescence intensity of UVB-exposed cells was markedly increased relative to controls. Conversely, RA could significantly decrease DPPP intensity (Fig. 2D), consistent with the results obtained from the 8-isoprostane measurement.

RA suppresses UVB-induced apoptosis

We then exposed human HaCaT keratinocytes to either RA alone, UVB alone, or pre-treatment with RA, followed by UVB exposure. MTT assay was used to evaluate the effect of treatments on cell viability. The results showed that UVB exposure caused a significant reduction in cell viability (Fig. 3A). When cells were pre-incubated with 2.5 μM RA, the loss of cell viability induced by UVB was significantly reduced. RA alone had no noticeable effect on cell viability. Similar results were observed after treatment with NAC following UVB exposure, relative to treatment with UVB alone.

Then we assessed the effect of RA against UVB radiation-induced apoptosis in human keratinocytes. Control cells and cells treated with RA alone contained mostly intact nuclei, whereas UVB-irradiated cells contained large numbers of apoptotic bodies, which indicate the occurrence of programmed cell death. The number of apoptotic bodies was dramatically reduced in UVB-irradiated cells pre-treated with RA

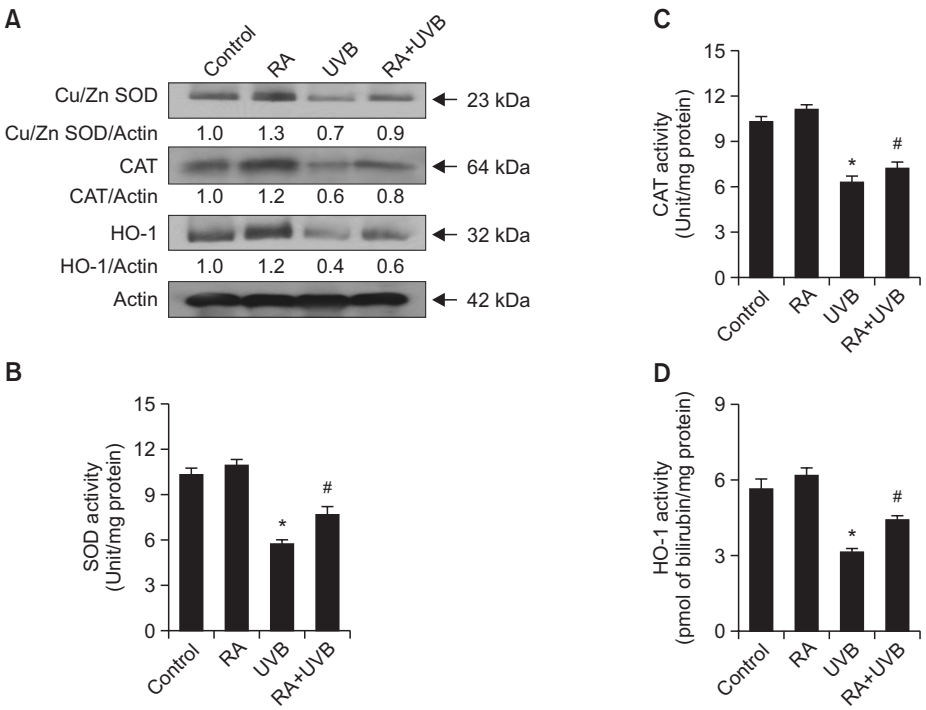

Fig. 4. RA enhances antioxidant systems decreased by UVB radiation. HaCaT cells were treated with 2.5 μM RA for 1 h, and then exposed to UVB radiation. (A) Cell lysates were subjected to gel electrophoresis, and then Western blot analysis was performed using antibodies against Cu/Zn SOD, CAT, and HO-1. Actin was used as a loading control. (B) and (C) SOD activity and CAT activity were expressed as the average enzyme U/mg protein ± SE. (D) HO-1 activity was expressed as pmol of bilirubin/mg protein ± SE. *Significant different from control cells (p<0.05); #significantly different from UVB-irradiated cells (p<0.05). (E) The cell lysates were Western blotted with antibody against Nrf2. (F) Confocal imaging using FITC-conjugated secondary antibody staining indicates the location of Nrf2 (green) by Nrf2 antibody, DAPI staining indicates the location of the nucleus (blue), and the merged image in RA-treated cells indicates the nuclear location of Nrf2 protein.

(Fig. 3B). These results were consistent with those obtained in cells pre-treated with 1 mM NAC, a well-known antioxidant that can reduce oxidative stress. In addition, UVB irradiation induced DNA fragmentation in human keratinocytes; however, treatment of the cells with RA suppressed DNA fragmentation, thereby preventing activation of apoptosis (Fig. 3C).

Effect of RA on the antioxidant system

We next investigated the defensive role of RA in regard to antioxidant systems. First, we conducted Western blot analyses to monitor the expression of antioxidant enzyme proteins. As shown in Fig. 4A, RA increased the protein expression of Cu/Zn SOD, CAT, and HO-1. UVB irradiation decreased the expression of these proteins; however, treatment with RA reversed this effect relative to UVB-treated cells. In addition, to determine whether the free-radical scavenging activity of RA was related to the cellular antioxidant systems, we assessed the activities of SOD, CAT, and HO-1. In UVB-irradiated cells, the activities of SOD, and CAT, showed comparatively lower superoxide anion and hydrogen peroxide inhibition than control cells (Fig. 4B, C). At the same time, UVB-irradiated cells were characterized by significantly lower level of HO-1 enzyme activity. However, pre-treatment with RA remarkably increased it in UVB-irradiated cells (Fig. 4D). Nrf2 is a main transcription factor that regulates SOD, CAT, and HO-1 gene expression. UVB-irradiated cells were significantly lower level of Nrf2 expression and translocation into nucleus, however, RA attenuated it (Fig. 4E, F).

DISCUSSION

Solar UV radiation is a potent environmental risk factor for non-melanoma skin cancer and accounts for several other harmful responses, including erythema, immunosuppression, edema, sunburn, hyperplasia, hyperpigmentation, and premature aging (Song and Gao, 2014). Keratinocytes are the predominant type of cell in the basal layer of the skin. UVB acts primarily on the epidermal basal cell layer, where it is absorbed by chromopores such as DNA, RNA, proteins, and melanin (Hojo *et al*., 1999; Mittal *et al*., 2003). This study demonstrated that RA can protect HaCaT keratinocytes against ROS, either generated by H_2O_2 or UVB exposure, providing convincing evidence that RA could play an important role in ROS scavenging.

UVB radiation is engaged in a critical role in apoptosis of human keratinocytes (Veratti *et al*., 2011). Therefore, we focused our experiments on determining the biophysical mechanism by which RA protects human keratinocytes against UVB-induced apoptosis. Due to similarities in structure and absorbance spectrum profiles between polyphenolic compounds and organic UV filters, polyphenols might be effective in photo-protection (Vostalova *et al*., 2010). RA was absorbed efficiently within the UVB range (280-320 nm) (data not shown). Therefore, it is reasonable to speculate that part of the cytoprotective effect of RA is due to direct absorption and scattering of UVB radiation. Moreover, treatment with RA prior to UVB irradiation significantly increased the viability of

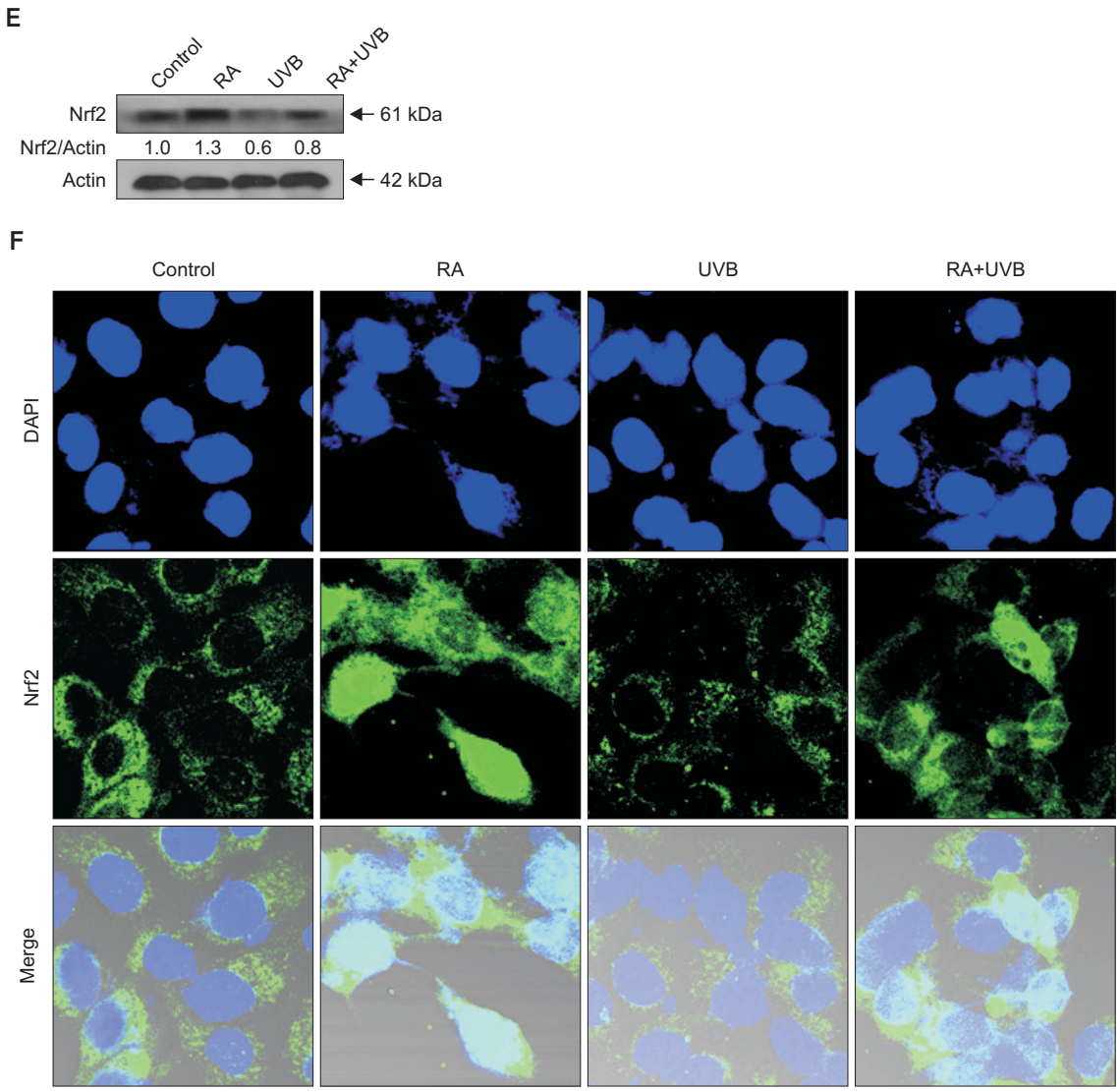

Fig. 4. Continued.

HaCaT cells. At the same time, pre-treatment with RA was followed by a significant reduction in DNA fragmentation and impaired formation of apoptotic bodies, highlighting the cytoprotective efficacy of RA against UVB-provoked apoptosis.

Many biological events, including physiological and non-physiological processes, trigger the generation of ROS (Andreyev *et al*., 2005; Balaban *et al*., 2005). These ROS, if generated in excess and not eliminated in a timely manner, can cause extensive oxidative damage to all types of biological macromolecules, including DNA, RNA, lipid, and protein. The cellular response induced by DNA damage is crucial for cell maintenance and cell fate (Jackson and Bartek, 2009). Our data show that RA attenuates UVB-induced macromolecular damage in human keratinocytes, and thus exerts potent therapeutic and chemopreventive effects related to UVB-induced carcinogenic processes.

Enzymatic and non-enzymatic antioxidants present in human skin prevent the adverse effects and alteration induced by levels of toxic exogenous/endogenous ROS. In this study, we revealed the cytoprotective mechanism of RA against oxidative stress induced by UVB by assessing the status of various antioxidant enzymes including SOD, CAT, and HO-1. SOD dismutates toxic superoxide into the less reactive H_2O_2, representing the first line of defense against free radicals. In this study, we found that protein level of cytosolic Cu/Zn SOD was significantly reduced in UVB-treated cells, leading to a corresponding decrease in SOD activity, whereas pre-incubation with RA (2.5 μM) recovered both SOD protein expression and activity. CAT, another prominent antioxidant protein, catalyzes the decomposition of H_2O_2 to water. HO-1 protects against a wide array of harmful stimuli, such as UV radiation, lipopolysaccharide, hyperoxia, and heme-induced damage (Motterlini *et al*., 2000; Fujii *et al*., 2003). Protein expression and enzyme activity of SOD, CAT and HO-1 were markedly reduced in UVB-treated cells. Meanwhile, pre-treatment with RA rescued SOD, CAT and HO-1 protein expression and enzyme activity suppressed by UVB radiation.

The transcription factor nuclear factor (erythroid-derived 2)-

like 2 (Nrf2) is referred to as the master regulator of the antioxidant response, modulating the expression of many antioxidant enzymes (Hybertson *et al*., 2011). Accumulation of Nrf2 in the nucleus permits its binding to the antioxidant-response element or electrophile-response element in the regulatory sequences of its target genes (Tkachev *et al*., 2011). The present data shows that RA treatment recovered the protein expression levels of Nrf2 decreased by UVB exposure, and resulted in the translocation of Nrf2 protein from the cytosol into the nucleus. These results indicate that RA may protect cellular environments from free-radical damage and thereby, enhance the cellular antioxidant defense system.

To summarize, the cytoprotective activity of RA against UVB radiation may be associated with elimination of ROS, which attenuates oxidative damage to cellular components and induction of apoptosis. Therefore, RA could be used as a therapeutic reagent to safeguard the skin from the deleterious effects of UVB irradiation. These findings may provide an experimental platform for further studies aimed at examining the bioavailability and photo-protective activity of RA, *in vitro* and *in vivo*, and determining their underlying mechanisms.

ACKNOWLEDGMENTS

This research was supported by the 2015 scientific promotion program funded by Jeju National University.

REFERENCES

Andreyev, A. Y., Kushnareva, Y. E. and Starkov, A. A. (2005) Mitochondrial metabolism of reactive oxygen species. *Biochemistry* **70**, 200-214.

Avila, A. J. G., Espinosa, G. A. M., De Maria, Y. C. D. M., Benitez, F. J. C., Hernández, D. T., Flores, M. S., Campos, C. J., Muñoz, L. J. L. and García, B. A. M. (2014) Photoprotection of *Buddleja cordata* extract against UVB-induced skin damage in SKH-1 hairless mice. *BMC Compelemt. Altern. Med.* **14**, 281-289.

Balaban, R. S., Nemoto, S. and Finkel, T. (2005) Mitochondria, oxidants, and aging. *Cell* **120**, 483-495.

Beauchamp, M. C., Letendre, E. and Renier, G. (2002) Macrophage lipoprotein lipase expression is increased in patients with heterozygous familial hypercholesterolemia. *J. Lipid Res.* **43**, 215-222.

Carmichael, J., DeGraff, W. G., Gazdar, A. F., Minna, J. D. and Mitchell, J. B. (1987) Evaluation of a tetrazolium-based semiautomated colorimetric assay: assessment of chemosensitivity testing. *Cancer Res.* **47**, 936-942.

Carrillo, M. C., Kanai, S., Nokubo, M. and Kitani, K. (1991) (-) deprenyl induces activities of both superoxide dismutase and catalase but not of glutathione peroxidase in the striatum of young male rats. *Life Sci.* **48**, 517-521.

Dean, R. T., Fu, S., Stocker, R. and Davies, M. J. (1997) Biochemistry and pathology of radical-mediated protein oxidation. *Biochem. J.* **324**, 1-18.

Fujii, H., Takahashi, T., Nakahira, K., Uehara, K., Shimizu, H., Matsumi, M., Morita, K., Hirakawa, M., Akagi, R. and Sassa, S. (2003) Protective role of heme oxygenase-1 in the intestinal tissue injury in an experimental model of sepsis. *Crit. Care Med.* **31**, 893-902.

Hanson, K. M. and Clegg, R. M. (2002) Observation and quantification of ultraviolet-induced reactive oxygen species in ex vivo human skin. *Photochem. Photobiol.* **76**, 57-63.

Hojo, M., Morimoto, T., Maluccio, M. and Asano, T. (1999) Cyclosporin induces cancer progression by a cell-autonomous mechanism. *Nature* **397**, 530-534.

Horiguchi, M., Masumura, K. I., Ikehata, H., Ono, T., Kanke, Y. and Nohmi, T. (2001) Molecular nature of ultraviolet B light-induced deletions in the murine epidermis. *Cancer Res.* **61**, 3913-3918.

Hybertson, B. M., Gao, B., Bose, S. K. and McCord, J. M. (2011) Oxidative stress in health and disease: the therapeutic potential of Nrf2 activation. *Mol. Aspects Med.* **32**, 234-246.

Jackson, S. P. and Bartek, J. (2009) The DNA-damage response in human biology and disease. *Nature* **461**, 1071-1078.

Kohno, M., Mizuta, Y., Kusai, M., Masumizu, T. and Makino, K. (1994) Measurements of superoxide anion radical and superoxide anion scavenging activity by electron spin resonance spectroscopy coupled with DMPO spin trapping. *Bull. Chem. Soc. Jpn.* **67**, 1085-1090.

Kutty, R. K. and Maines, M. D. (1982) Oxidation of heme c derivatives by purified heme oxygenase. Evidence for the presence of one molecular species of heme oxygenase in the rat liver. *J. Biol. Chem.* **257**, 9944-9952.

Lee, H. J., Cho, H. S., Park, E., Kim, S., Lee, S. Y. and Kim, C. S. (2008) Rosmarinic acid protects human dopaminergic neuronal cells against hydrogen peroxide-induced apoptosis. *Toxicology* **250**, 109-115.

Lee, K. O., Kim, S. N. and Kim, Y. C. (2014) Anti-wrinkle effects of water extracts of teas in hairless mouse. *Toxicol Res.* **30**, 283-289.

Li, L., Abe, Y., Kanagawa, K., Usui, N., Imai, K., Mashino, T., Mochizuki, M. and Miyata, N. (2004) Distinguishing the 5,5-dimethyl-1-pyrroline N-oxide (DMPO)-OH radical quenching effect from the hydroxyl radical scavenging effect in the ESR spin-trapping method. *Anal. Chim. Acta* **512**, 121-124.

McArdle, F., Rhodes, L. E., Parslew, R., Jack, C. I. A., Friedmann, P. S. and Jackson, M. J. (2002) UVR-induced oxidative stress in human skin in vivo: effects of oral vitamin C supplementation. *Free Radic. Biol. Med.* **33**, 1355-1362.

Misra, H. P. and Fridovich, I. (1972) The role of superoxide anion in the autoxidation of epinephrine and a simple assay for superoxide dismutase. *J. Biol. Chem.* **247**, 3170-3175.

Mittal, A., Elmets, C. A. and Katiyar, S. K. (2003) Dietary feeding of proanthocyanidins from grape seeds prevents photocarcinogenesisin SKH-1 hairless mice: Relationship to decreased fatand lipid peroxidation. *Carcinogenesis* **24**, 1379-1388.

Motterlini, R., Foresti, R., Bassi, R., Calabrese, V., Clark, J. E. and Green, C. J. (2000) Endothelial heme oxygenase-1induction by hypoxia. Modulation by inducible nitric-oxidesynthase and S-nitrosothiols. *J. Biol. Chem.* **275**, 13613-13620.

Okimoto, Y., Watanabe, A., Niki, E., Yamashita, T. and Noguchi, N. (2000) A novel fluorescent probe diphenyl-1-pyrenylphosphine to follow lipid peroxidation in cell membranes. *FEBS Lett.* **474**, 137-140.

Park, H. M., Kim, H. J, Jang, Y. P. and Kim, S. Y. (2013) Direct analysis in real time mass spectrometry (DART-MS) analysis of skin metabolome changes in the ultraviolet B-induced mice. *Biomol. Ther.* **21**, 470-475.

Perez-Sanchez, A., Barrajon-Catalan, E., Caturla, N., Castillo, J., Benavente-Garcia, O., Alcaraz, M. and Micol, V. (2014) Protective effects of citrus and rosemary extracts on UV-induced damage in skin cell model and human volunteers. *J. Photochem. Photobiol. B.* **136**, 12-18.

Piao, M. J., Kang, K. A., Kim, K. C., Chae, S., Kim, G. O., Shind, T., Kim, H. S. and Hyun, J. W. (2013) Diphlorethohydroxycarmalol attenuated cell damage against UVB radiation via enhancing antioxidant effects and absorbing UVB ray in human HaCaT keratinocytes. *Environ.Toxicol. Pharmacol.* **36**, 680-688.

Rosenkranz, A. R., Schmaldienst, S., Stuhlmeier, K. M., Chen, W., Knapp, W. and Zlabinger, G. J. (1992) A microplate assay for the detection of oxidative products using 2',7'-dichlorofluorescin-diacetate. *J. Immunol. Methods* **156**, 39-45.

Silva, A. R., Menezes, P. F. C., Martinello, T., Novakovich, G. F. L., De Oliveira P. C. E. and Feferman, I. H. S. (2010) Antioxidant kinetics of plant-derived substances and extracts. *Int. J. Cosmet. Sci.* **32**, 73-80.

Singh, N. P. (2000) Microgels for estimation of DNA strand breaks, DNA protein crosslinks and apoptosis. *Mutat. Res.* **455**, 111-127.

Song, J. L. and Gao, Y. (2014) Protective effects of *Lindera coreana* on UVB-induced oxidative stress in human HaCaT keratinocytes. *Iran J. Pharm. Res.* **13**, 1369-1378.

Tkachev, V. O., Menshchikova, E. B. and Zenkov, N.K. (2011) Mechanism of the Nrf2/ Keap1/ ARE signaling system. *Biochemistry* **76**, 407-422.

Vayalil, P. K., Mittal, A., Hara, Y., Elmets, C. A. and Katiyar, S. K. (2004) Green tea polyphenols prevent ultraviolet light-induced oxidative damage and matrix metalloproteinases expression in mouse skin. *J. Invest. Dermatol.* **122**, 1480-1487.

Veratti, E. I., Rossi, T., Giudice, S., Benassi, L., Bertazzoni, G., Morini, D., Azzoni, P., Bruni, E., Giannetti, A. and Magnoni, C. (2011) 18beta-glycyrrhetinic acid and glabridin prevent oxidative DNA fragmentation in UVB-irradiated human keratinocyte cultures. *Anticancer Res.* **31**, 2209-2215.

Verschooten, L., Claerhout, S., Laethem, A. V., Agostinis, P. and Garmyn, M. (2006) New strategies of photoprotection. *Photochem. Photobiol.* **82**, 1016-1023.

Vostalova, J., Zdarilova, A. and Svobodova, A. (2010) *Prunella vulgaris* extract and rosmarinic acid prevent UVB-induced DNA damage and oxidative stress in HaCaT keratinocytes. *Arch. Dermatol. Res.* **302**, 171-181.

Yoshihisa, Y., Rehman, M. U. and Shimizu, T. (2014) Astaxanthin, a xanthophyll carotenoid, inhibits ultraviolet-induced apoptosis in keratinocytes. *Exp. Dermatol.* **23**, 178-183.